Kinetics and morphologies of viscoelastic phase separation

Jianing Zhang, Zhenli Zhang, Hongdong Zhang, and Yuliang Yang*
Department of Macromolecular Science, Ministry's Key Lab of Molecular Engineering of Polymers, SMEC, Fudan University, Shanghai 200433, China

(Received 22 March 2001; published 30 October 2001)

In this paper, the effects of relaxational bulk modulus and the average composition of polymers on the viscoelastic phase separation are investigated in detail. It is found that there are two typical morphologies, i.e., moving droplet phase and phase inversion, and the relaxation of the dynamical asymmetry and the amplification of the concentration fluctuation are responsible for the appearance and evolution of different morphologies of viscoelastic phase separation. It is found that, for the viscoelastic phase separation, the scattering function has two peaks. The growth exponents of the main and the secondary peaks in the late stage are almost the same and ~0.6, which also agrees with the experimental observations. On the other hand, the growth exponent of the secondary peak increased from ~0.42 to ~0.66 with increase of ϕ_0 from 0.275 to 0.4, in the intermediate stage.

DOI: 10.1103/PhysRevE.64.051510 PACS number(s): 64.75.+g, 61.25.Hq, 47.20.Hw, 05.70.Fh

I. INTRODUCTION

In recent years, there has been an increasing interest in investigating the viscoelastic effects in phase separation. The viscoelastic effects on the early stage of phase separation were first analyzed by de Gennes [1], and later by Doi and Onuki [2], Onuki [3], Onuki and Taniguchi [4], and Kumaran and Fredrickson [5]. The effect of viscoelasticity on the shear-induced phase separation has also been discussed [2,6] and it is found that it gives rise to nonexponential decay in dynamic light scattering [2]. Recently, a quite unusual phase separation was found in polymer systems having intrinsic dynamic asymmetry between two components. This asymmetry in molecular dynamics between two components leads to the strong kinetic coupling between the stress field and the concentration fluctuation. Such a phase separation is called ''viscoelastic phase separation'' [7], since viscoelastic effects play a crucial role in addition to diffusion and hydrodynamic effects.

Although there have been some experiments investigating viscoelastic phase separation [8–11], the computer simulations with regard to this are still not abundant. The simulations of Sappelt and Jäckle [12] and Ahluwalia [13] are based on a solid model (model B) which seems not really suitable for the viscoelastic phase separation. In the simulation of Ahluwalia [13], the dynamic asymmetry is incorporated by introducing a function of order parameter-dependent mobility. Clarke *et al.* [14] and Cao *et al.* [15] have also investigated the viscoelastic effect on the kinetics and morphology for polymer blends through introducing a relaxing elastic term into the free energy functional and the simulations based on the time-dependent Ginzburg-Landau (TDGL) equation. However, including the dynamical asymmetry in the diffusion constant or incorporating the viscoelastic effects in the mixing free energy function is inappropriate and not straightforward since the relaxation nature of stress should be incorporated in mechanical stresses constitutive equations and the fluid nature is essential for viscoelastic phase separation [16]. Taniguchi and Onuki [17], Tanaka and Araki [18], and Sagui *et al.* [19] have performed the simulations based on a two-fluids model developed by Doi and Onuki [2]. In the simulations of Taniguchi and Onuki, the viscoelastic contribution has been included by introducing a so-called conformation tensor. Although their study has clarified some essential features of viscoelastic phase separation, it is not able to see phase inversion observed in the experiments [17]. The viscoelastic model proposed by Tanaka [7], i.e., the model we used here, added a bulk relaxational modulus to the two-fluids model, which is more phenomenological but the eventual phase inversion can be observed.

So far, the quantitative studies on viscoelastic phase separation have just been initiated. In the simulations of Tanaka and Araki [18], only very few extreme cases were shown. Here, we would like to focus our special attention on the effects of relaxational bulk modulus and the average composition of polymer on the viscoelastic phase separation. Especially, we would like to study their effect on the domain growth exponents and the temporal relaxation of the bulk modulus. Therefore, we will illustrate how the bulk modulus and the average composition of polymer affect the phase separation kinetics, which is crucial for the understanding the universality of viscoelastic phase separation with phase inversion, moving droplet phase (MDP) [8,16]. We will show that the competition between the concentration fluctuation amplification and the relaxation of dynamical asymmetry may be the key determining whether phase inversion would happen.

The rest of the paper is organized as follows. In Sec. II, the viscoelastic model equations and the algorithm used in this work are briefly introduced. In Sec. III, the numerical results with various values of bulk modulus and average composition of polymer will be presented and discussed in detail. Section VI gives the summary of this paper.

II. MODEL AND SIMULATION ALGORITHM

In our simulation, the viscoelastic model of polymer solutions brought forward by Tanaka and Araki [18] is used.

*Author to whom the correspondence should be addressed.

The basic equations can be written as [2,18]

$$\frac{\partial \phi}{\partial t} = -\nabla \cdot (\phi \mathbf{v}) - \nabla \cdot [\phi(1-\phi)(\mathbf{v}_p - \mathbf{v}_s)],$$

$$\mathbf{v}_p - \mathbf{v}_s = -\frac{1-\phi}{\zeta}[\nabla \cdot \mathbf{\Pi} - \nabla \cdot \boldsymbol{\sigma}] = -\frac{1-\phi}{\zeta}\left[\phi \nabla\left(\frac{\partial f}{\partial \phi} - C\nabla^2 \phi\right) - \nabla \cdot \boldsymbol{\sigma}\right], \tag{1}$$

$$\rho \frac{\partial \mathbf{v}}{\partial t} \cong -\nabla \cdot \mathbf{\Pi} + \nabla p + \nabla \cdot \boldsymbol{\sigma} + \eta_s \nabla^2 \mathbf{v},$$

where ζ is the friction coefficient of order $6\pi\eta_0 b^{-2}\phi^2$, b being the monomer size. C describes the strength of the interfacial free energy and is set equal to $(kT/\nu_m)C_0/\phi$, where ν_m is the volume of a monomer, p is the pressure, η_s is the viscosity of the solvent and is taken to be $\zeta C_0/\phi^2$. Space and time is in the unit of $l=(NC_0)^{1/2}/4$ and $\tau_0 = (\nu_m N^{1/2}/kT)(\zeta/\phi^2)l^2$ [17]. All the quantities have been made dimensionless in Eq. (1), the form of which is similar to model H except the introduction of the force balance equation and network force term, $\phi(\mathbf{r},t)$ is the volume fraction of polymer at position $\mathbf{r}$ and time t, while $\mathbf{v}_p$ and $\mathbf{v}_s$ are the velocities of polymer and solvent, respectively. The average velocity $\mathbf{v}$ is defined as $\mathbf{v}=\phi\mathbf{v}_p+(1-\phi)\mathbf{v}_s$, and f is the Flory-Huggins free energy [20],

$$\frac{f(\phi)}{kT} = \frac{1}{N}\phi \ln \phi + (1-\phi)\ln(1-\phi) + \chi\phi(1-\phi), \tag{2}$$

where N is the chain length of the polymer. In this study, as adopted by Tanaka and Araki [18], we set $N=1$ and do not introduce any dependence of C on ϕ to pick up the pure effect of dynamic asymmetry. The components of the total stress $\boldsymbol{\sigma}$ is defined as

$$\sigma_{ij} = \int_{-\infty}^{t} dt' \left[G(t-t')\left(\frac{\partial \nu_P^j}{\partial x_i} + \frac{\partial \nu_p^i}{\partial x_j} - \frac{2}{d}(\nabla \cdot \mathbf{v}_P)\delta_{ij}\right) + K(t-t')\nabla \cdot \mathbf{v}_p(t')\delta_{ij}\right], \tag{3}$$

where d is the spatial dimensionality, K and G are the bulk and shear relaxation moduli that are assumed to be of Maxwell type,

$$K(t) = M_b \exp(-t/\tau_b), \quad G(t) = M_s \exp(-t/\tau_s). \tag{4}$$

The second term on the right-hand side of Eq. (3) has been introduced to incorporate the effect of volume change into the stress tensor and its diagonal nature leads to the direct coupling with diffusion. In our simulation, the parameters, M_b, M_s, τ_b, and τ_s are functions of ϕ only, i.e.,

$$M_b = M_b^0 \theta(\phi - \phi_0); \quad M_s = M_s^0 \phi^2 \tag{5}$$

and

$$\tau_b = \tau_b^0 \phi^2; \quad \tau_s = \tau_s^0 \phi^2, \tag{6}$$

where ϕ_0 is the average composition of polymer in the mixture, $\theta(\phi-\phi_0)$ is the step function that equals 1.0 when ϕ is larger than ϕ_0 while equals zero when ϕ is smaller than ϕ_0. In this simulation, we set $\gamma_b^0=10$, $\tau_s^0=50$, and $M_s^0=0.5$. So, the shear relaxation modulus is assumed to be $M_s = 0.5(kT/v_m)\phi^2$ and the shear relaxation time to be $\tau_s = 50\tau_0\phi^2$. The corresponding bulk parts are analogous and they are all made dimensionless in Eqs. (5) and (6). It should be pointed out that the above functional forms of the moduli are rather artificial since the theoretical prediction of them under a poor polymer solution condition, where phase separation occurs, is still quite difficult and not available so far [7,16]. Tanaka and Araki [7] speculate that polymer solution behaves as a physical gel universally at least at a higher polymer solution concentration under a strongly poor solvent condition. They introduce the dynamical asymmetry by choosing the above composition dependence of M_b to produce the sudden change of $K(t)$ from $K(t)\cong 0$ to that of a transient gel, $K(t)\cong K_{tg}$ [7]. At the same time, we may stress that the sudden change in M_b is similar to the sharp step function of the mobility in Ref. [13]. Although there is no firm basis on the above relations assumed in Eqs. (5) and (6), the details of dependences of these quantities on ϕ do not affect the qualitative features of the simulated results [18]. The physical relevance of the above forms of the moduli was discussed in more detail in Refs. [7] and [16]. A more relevant microscopic theory of polymer solution in a poor solution condition, where phase separation occurs, is highly desirable.

In our simulation, we solve the following upper-convective equations instead of Eq. (3):

$$\frac{\partial \boldsymbol{\sigma}_s}{\partial t} + \mathbf{v}_p \cdot \nabla \boldsymbol{\sigma}_s = \nabla \mathbf{v}_p \cdot \boldsymbol{\sigma}_s + \boldsymbol{\sigma}_s \cdot (\nabla \mathbf{v}_p)^T - \frac{1}{\tau_s}\boldsymbol{\sigma}_s + M_s[\nabla \mathbf{v}_p + (\nabla \mathbf{v}_p)^T], \tag{7a}$$

$$\frac{\partial \sigma_b}{\partial t} + \mathbf{v}_p \cdot \nabla \sigma_b = -\frac{1}{\tau_b}\sigma_b + M_b \nabla \cdot \mathbf{v}_p. \tag{7b}$$

Since the bulk stress is isotropic, in obtaining Eq. (7b) the fact that σ_b is a scalar variable has been used. Therefore, we have $\boldsymbol{\sigma}_b = \sigma_b \mathbf{I}$ or $\sigma_b = 1/d\ \mathrm{Tr}\ \boldsymbol{\sigma}_b$ [7]. Since the shear stress is a traceless tensor, we calculate the final form of shear stress as $\boldsymbol{\sigma}_s^f = \boldsymbol{\sigma}_s - 1/d\ \mathrm{Tr}(\boldsymbol{\sigma}_s)\mathbf{I}$, where $\mathbf{I}$ is a unit tensor and d is the space dimensionality. Hereafter, we denote this final stress $\boldsymbol{\sigma}_s^f$ as $\boldsymbol{\sigma}_s$. Then we calculate the total stress $\boldsymbol{\sigma}$ as $\boldsymbol{\sigma} = \boldsymbol{\sigma}_s + \boldsymbol{\sigma}_b$. All the three quantities are reused in the next iteration. Introducing the bulk part into the stresses constitutive equation naturally incorporated the dynamical asymmetry into viscoelastic phase separation by the composition dependence of the bulk moduli with a sharp step function form.

The detailed simulation algorithm is exactly the same as that proposed by Tanaka and Araki [18]. Therefore, we only briefly introduce the simulation algorithm. The above Langevin equations were simulated numerically by the Euler method in two dimensions ($d=2$) using periodic boundary conditions, under the incompressibility condition $\nabla \cdot \mathbf{v} = 0$

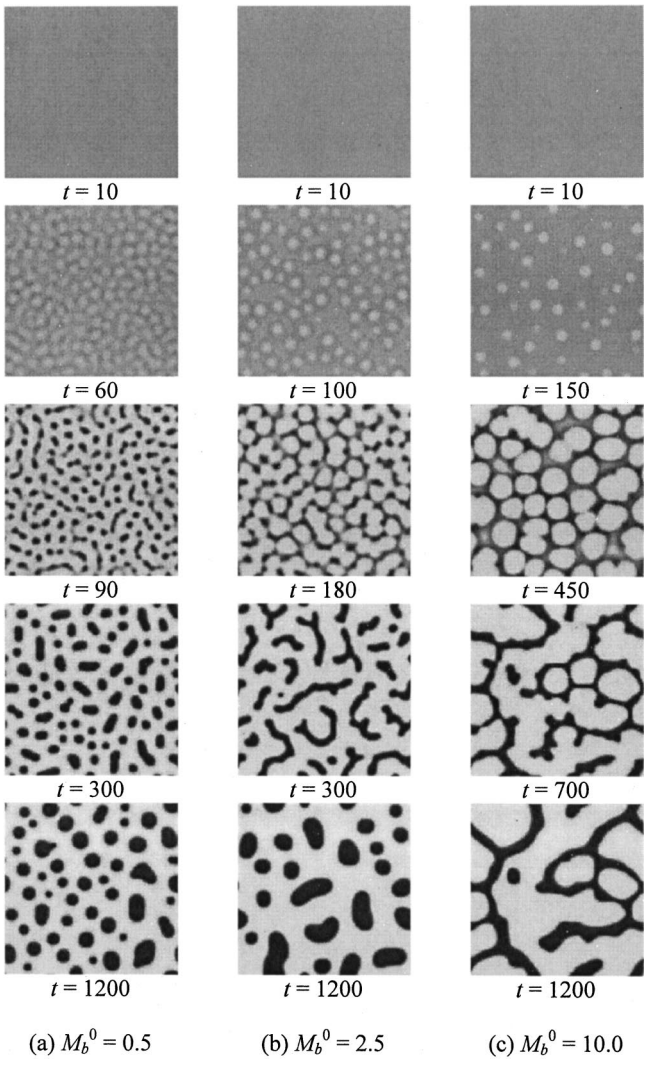

FIG. 1. The morphological evolutions obtained for various values of M_b^0 for the average composition of polymer $\phi_0 = 0.35$.

and the quasistationary approximation $\partial \mathbf{v}/\partial t \cong 0$. The system size was 128×128 and the grid size $\Delta x = \Delta y = 1$ and the time step is $\Delta t = 0.02$. The other parameters are: $\eta_s = 0.1$, $\zeta = 0.1$, $kT = 1.3$, and $\chi = 2.7$. The Gaussian random noise of ϕ with intensity of 10^{-3} is introduced into the initial composition distribution.

III. RESULTS AND DISCUSSIONS

A. The effect of bulk modulus on the morphology of viscoelastic phase separation

Figure 1 shows the morphological evolution of viscoelastic phase separation for $\phi_0 = 0.35$ with various extent of dynamic asymmetry. The dynamic asymmetry between the polymer-rich phase and solvent-rich phase is introduced by Eq. (5) with M_b^0 varying from zero to 10. Therefore, the extent of dynamical asymmetry is enhanced in company with the aggrandizement of M_b^0. In the excessive situation when M_b^0 is approximately equal to zero, i.e., dynamical symmetry

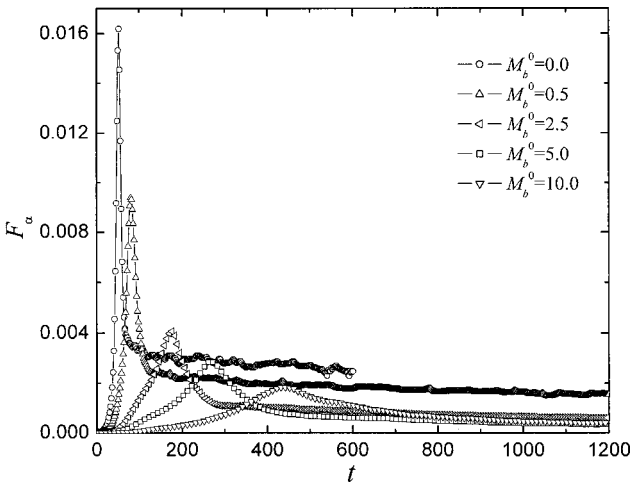

FIG. 2. The evolution of the apparent thermodynamic force F_α as a function of M_b^0.

case, we get the usual phase separation that is similar to the case showed in Fig. 1(a) if the existence of shear relaxation modulus is ignored (i.e., $M_s^0 = 0$).

It is seen from Fig. 1 that the phase inversion morphologies are observed when increasing the value of M_b^0. The phase inversion process can be described as follows: The solvent-rich droplets dispersed in the polymer-rich matrix appear first. Then, these droplets are growing up and the area of the polymer-rich phase is becoming smaller and smaller, the polymers are then more and more enriched in the area between the droplets. Therefore, the network like polymer-rich phase is formed. As the time passes, the polymer-rich network breaks up and shrinks into the polymer-rich droplets in order to reduce the surface tension. Finally, the morphology, that the polymer-rich droplets are dispersed in the solvent-rich matrix, was formed, Fig. 1(b).

Figure 2 shows the temporal change in the average magnitudes per lattice of the apparent thermodynamic force $F_\alpha = |\nabla \cdot \mathbf{\Pi} - \nabla \cdot \boldsymbol{\sigma}|$ with the augmentation of bulk modulus. The corresponding pattern evolution is shown in Fig. 1. It is seen that all the evolution curves show a peak that reflects the increase in the coupling between the diffusion fields around the solvent-rich droplets [18]. With M_b^0 increasing, the apparent thermodynamical force F_α as well as the peak value is reduced and retarded. At the same time, the competition between the concentration fluctuation amplification and the relaxation of dynamical asymmetry results in the crossover from a morphology of transient polymer-rich network [Fig. 1(b)] to forming a morphology of longtime network domains [Fig. 1(c)] [17]. It can be seen from Fig. 2 that the augmentation of F_α becomes slackened with the increase of M_b^0 in the early stage, which correspond with the prolongation of the ''frozen period.'' It can also be seen that the equilibrium value of F_α in the late stage exists.

Figure 3 shows the temporal change of the area fraction of polymer-rich phase (ϕ_{area}) in the viscoelastic phase separation. By comparing Fig. 3 with Fig. 1, it is seen that, in the very early stage, the homogeneous phase discharged the solvent due to the thermodynamical force and became the

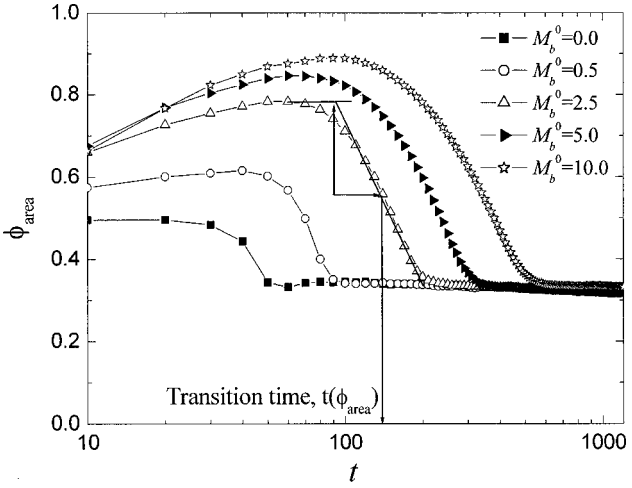

FIG. 3. The evolution of the area fraction of the polymer-rich phase for various values of M_b^0.

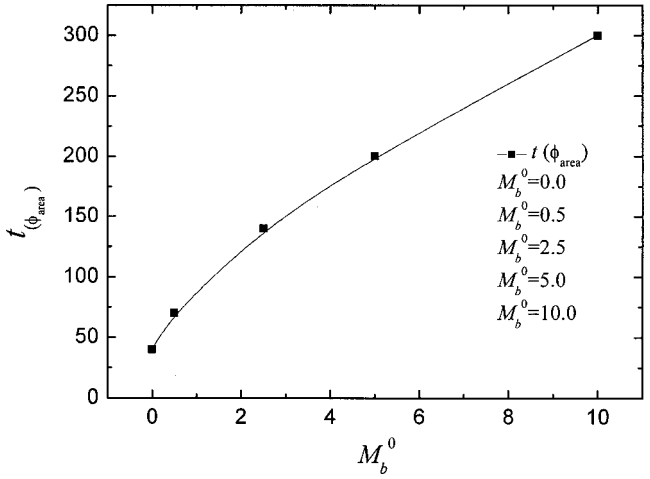

FIG. 4. The transition time for the phase inversion obtained from the results shown in Fig. 3. The transition time is defined in Fig. 3.

polymer-rich phase resulting in the augmentation of ϕ_{area}. Consequently, the solvent-rich droplets became more and more large and compressed the surrounded polymer-rich phase, which caused the decrease of ϕ_{area}. Since the modulus contrast between polymer-rich phase and solvent-rich phase exists, the stress is asymmetrically distributed to polymer-rich phase. The thin parts of network structure are compressed and ultimately broken, cf. Fig. 1(b). As M_b^0 increases, the bulk stress is strengthened while F_α decreases, Fig. 2, which inhibited the disconnection of network structure until the concentration fluctuation is amplified to the final equilibrium value. Although ϕ_{area} has dropped to 0.5 in the case $M_b^0=10$, there is no time for the phase inversion to happen and the network structure is maintained longer, Fig. 1(c). It is clearly seen in Fig. 3 that, as M_b^0 is increasing, the concentration fluctuation amplification is prolonged resulting in the volume shrink of polymer-rich phase even after the formation of a sharp interface, Figs. 1(b) and 1(c) [13,18]. The dynamical difference between the usual phase separation and phase inversion is also clarified in Fig. 4. The transition time for the phase inversion is obtained from the results shown in Fig. 3 by the following way. We first locate the peak position of the curve and give a middle-high horizontal line, the point of intersection between which and the original curve is approximately estimated as the transition time. From Fig. 4 we can see that the dynamical asymmetry aggrandizes and the kinetics of phase separation is postponed with the increase of M_b^0. When M_b^0 is close to 0 (i.e., dynamical symmetry case), the phase inversion could not be observed due to the reason of accelerated kinetics. Therefore, it should be pointed out that it is not M_s^0 but M_b^0 that leads to the forming of network domain structure [18]. However, the latter is responsible for the retaining of network.

The scattering function $S(k,t)$ of a typical viscoelastic phase separation is shown in Fig. 5. It is seen from Fig. 5 that the scattering function at early stage has one peak that corresponds to the scattering of the solvent-rich droplets. As the time passes, this main peak moves to the smaller k, meanwhile a secondary peak is appearing at larger k and merging into the main peak in the late time. The peak maxims, k_{m1} and k_{m2}, represent the characteristic size of solvent-rich phase and polymer-rich phase of network in turn. In the intermediate stage, both peaks grow in intensity and decreases in the wave number of the peak position with time. The second peak appears as a definite peak at first and seems to form a shoulder of the main peak finally. These simulated results of two scattering peaks agree with the experimental observations for the phase separation of polymer solution [21]. We designate the wave number of the maximum of the main and the secondary peaks as k_{m1} and k_{m2}, respectively. Figure 6 shows the evolution of these two peaks for a typical viscoelastic phase separation. It is seen that the system behaved as a dynamically symmetrical system when $M_b^0<0.25$, which is consistent with the results of Kuwahara and Kubota [21]. Following the study of Refs. [21] and [22], we here considered the evolution of peak maximum. From Fig. 6(a), it is seen that the early stage of spinodal decomposition predicted by Cahn's theory was

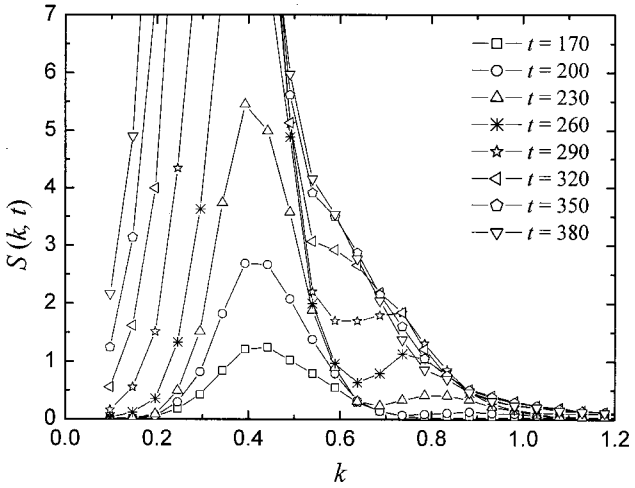

FIG. 5. The time evolution of the scattering function for a typical viscoelastic phase separation with $M_b^0=5.0$.

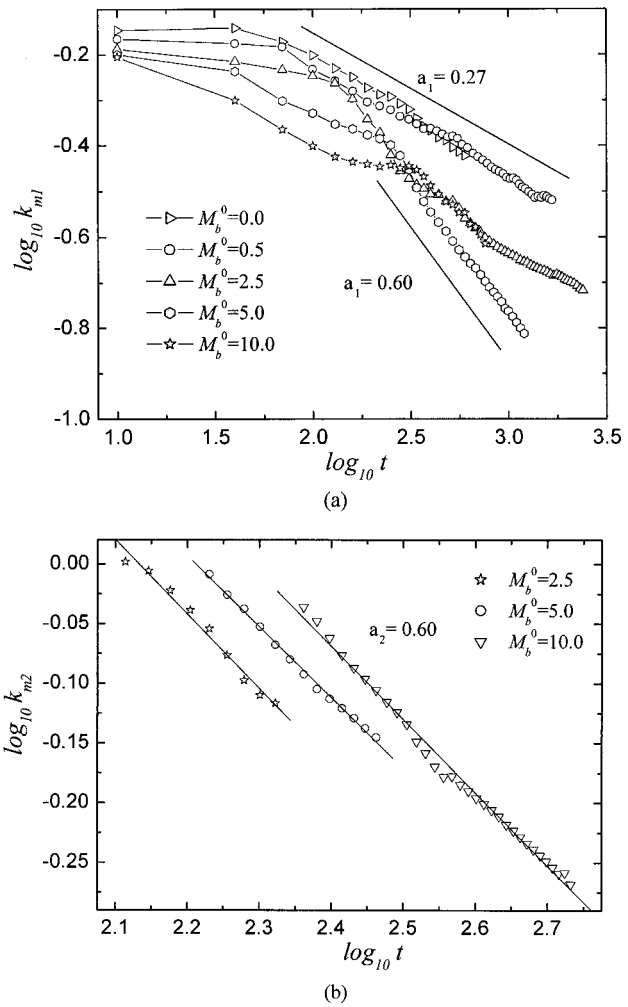

FIG. 6. (a) The evolution of the wave number of the first maximum of scattering function; (b) The evolution of the wave number of the second maximum of scattering function.

clearly observed. For the case of dynamical asymmetry (i.e., M_b^0 becomes larger), the growth exponent of the main peak α_1 in the late stage increases from $\sim$ 0.27 to $\sim$0.6. Figure 6(b) reveals that the growth exponent of the second peak α_2 seems to be a constant, $\alpha_2 \sim 0.6$. We should emphasize that the coalition of solvent-rich droplets will lead to an abnormal augmentation of α_1, which is neither practical growth of domain of polymer-rich phase nor solvent-rich phase. Due to the complexity of this process, the evolution curves of k_{m1}, do not look so regular. The time for the appearance of the second peak is retarded with the increase of M_b^0, which suggests that the origin of the second peak is probably the thin parts of network structure formed in the middle stage [22]. Due to the formation and breaking of the network like phase structure, the scaled scattering functions cannot be superimposed into a universal function at the early and intermediate stages, which reveals that the self-similarity does not exist, which agrees with the results obtained by Ahluwalia [13] and Cao *et al.* [15] cf. Fig. 7. In the very late stage, the network has been broken and the phase structure was almost frozen and then the scaled scattering functions could be superimposed [13,15].

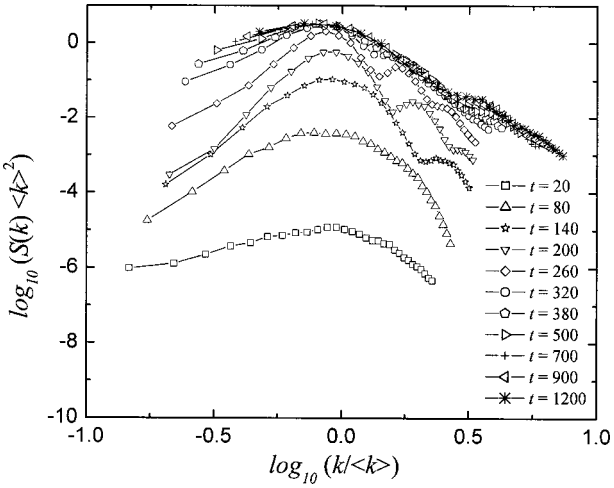

FIG. 7. The scaled scattering function shows that the self-similarity is only valid for very late stage of the phase separation ($M_b^0 = 5.0$).

B. The effect of bulk modulus on the relaxation of the modulus

The temporal relaxation processes of the modulus are shown in Fig. 8. Here we should mention that the bulk relaxation only happened in the polymer-rich phase due to the assumption of θ function in Eq. (5), i.e., $M_b = M_b^0 \theta(\phi - \phi_0)$. The retarding effect of the increase of M_b^0 is clearly seen. It is seen from Fig. 8 that, the relaxation process can be divided into two periods characterized by two straight lines in the log-log plot, which reveals the Maxwell relaxation nature in the early and late stages. During the first linear period, the morphology of solvent-rich droplets appears. In this period, the inverse relaxation time of $1/\tau_1$ is $\sim$0.35. It seems that $1/\tau_1$ is not related to the value of M_b^0 that only retards the transition to the second linear period. During the second linear period, the networklike morphology appears. In this period, the relaxation time is much longer, $1/\tau_2 \sim 0.054$. Comparing to the results shown in Fig. 14 that $1/\tau_2$ is independent of the average composition of polymer ϕ_0, it

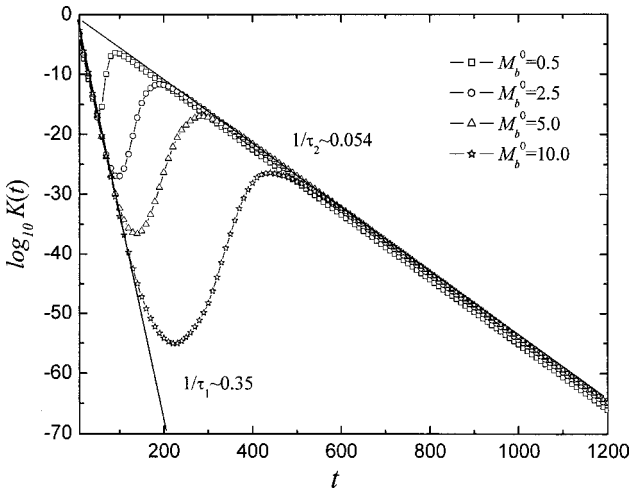

FIG. 8. The relaxation of the bulk modulus in the polymer-rich phase for various values of M_b^0.

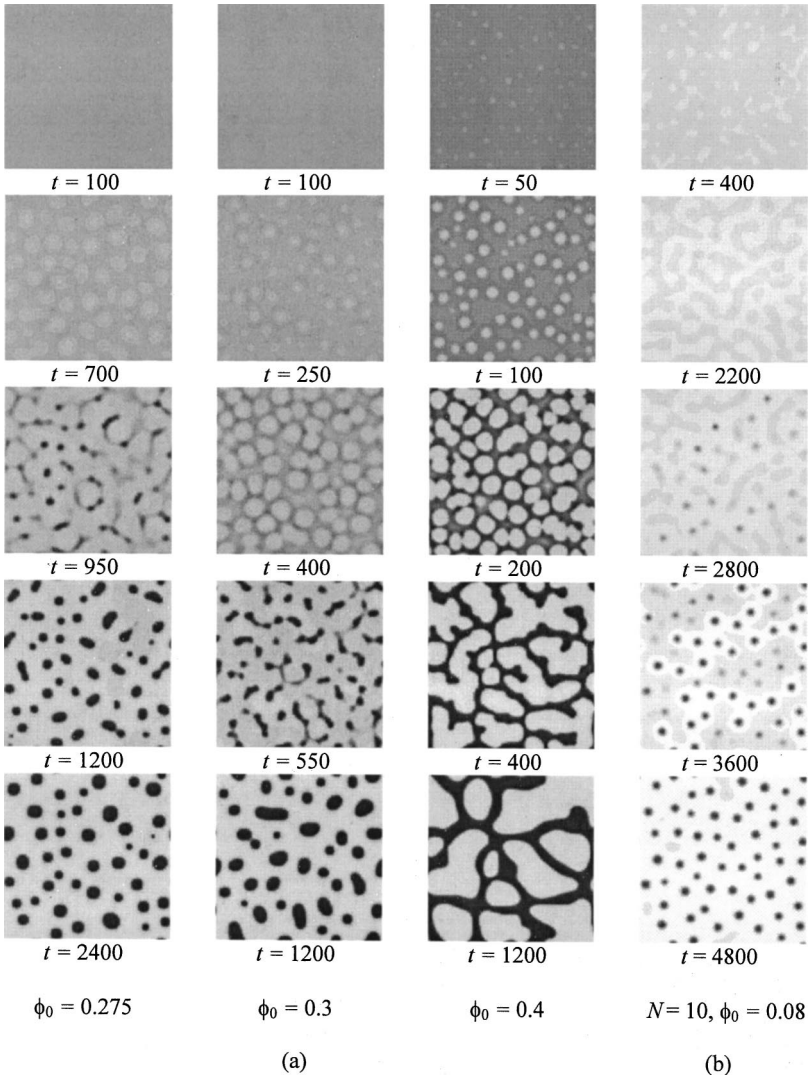

FIG. 9. (a) The morphological evolution of the viscoelastic phase separation for various average composition of polymer ϕ_0. The value of M_b^0 is fixed to be 5.0. (b) The schematic morphological evolution of MDP for the case of lower ϕ_0. The value of N is set to be 10, which is more coincident with experimental evidences.

can be concluded that this relaxation time only depends on the quenching depth, i.e., the equilibrium composition of the polymer-rich phase. It is known that, for the quenching depth of $\chi=2.7$, the equilibrium composition are 0.107 and 0.893 for the solvent-rich and polymer-rich phase, respectively. Thus, the final area fraction of the polymer-rich phase $\phi^e_{\text{area}}=0.309$. Therefore, following Eq. (6), in the late stage, the relaxation time should be estimated by $1/\tau_2 \propto 1/(\tau_b^0 \phi_e^2)$. However, in the first period, the system has not reached the phase equilibrium. Therefore, the area fraction and the composition of the polymer-rich phase have not reached the equilibrium value. In this period, Fig. 14 implies that the relaxation time of $1/\tau_1$ depends on the average composition of the polymers, ϕ_0. Therefore, $1/\tau_1$ for various ϕ_0 shown in Fig. 14 reveals its ϕ_0 dependence.

By comparing to the case of without viscoelastic effect, we can see that, in addition to the special networklike morphology, the viscoelastic effect actually prohibits the phase separation, which results in the retardation of the transition between these two periods. This picture is consistent with the general tendency of thermodynamic force F_a shown in Fig. 2, i.e., the transition of the bulk modulus relaxation happens when the thermodynamic force F_a reaches the maximum.

C. The effect of the average composition on the kinetics and morphology of viscoelastic phase separation

In order to investigate the effect of average composition of polymer on the kinetics and morphology of viscoelastic phase separation, we fix the $M_b^0=5.0$ while varying ϕ_0 from 0.275 to 0.4.

Figure 9(a) showed the morphological evolution for various ϕ_0. It is seen that, in the case of $\phi_0=0.3$, the complete course of phase inversion is observed. However, in the case of lower ϕ_0, the phase inversion of middle stage becomes very obscure and dynamics of phase separation is prolonged. We believe this picture is associated with the MDP also studied by Tanaka from theoretical and experimental viewpoints [8,9,16]. On the other hand, phase inversion will be retarded in the case of high ϕ_0 and a network domain structure will be kept longer, which is similar to the results in Ref. [17]. In our simulations, there is no evidence of the breakup of network into droplets (at least until $t=2400$ for $\phi_0=0.4$), which is consistent with the experimental observation in Ref. [22]. The reason may be that the polymer-rich phase has reached the final equilibrium concentration before the breakup of network. It should be mentioned that the magnitude of stress

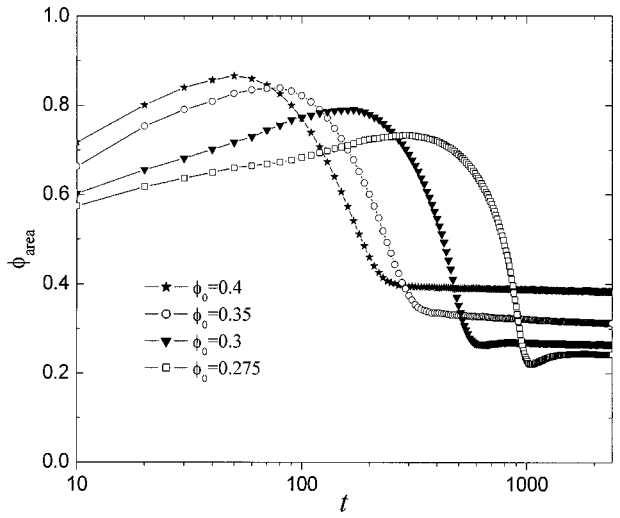

FIG. 10. The evolution of the area fraction of polymer-rich phase obtained for various values of the average composition of polymer, ϕ_0.

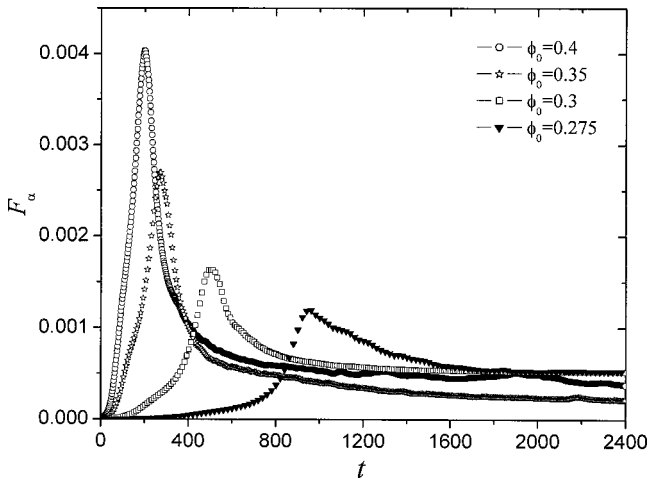

FIG. 11. The evolution of the apparent thermodynamic force F_α as a function of the average composition of polymer, ϕ_0.

force, $|\nabla\cdot\boldsymbol{\sigma}|$, is aroused from the thermodynamic force, $|\nabla\cdot\boldsymbol{\Pi}|$, and tends to counteract the effects of the latter. In simulation results, it will never surpass and relax synchronously with the latter to the final equilibrium value.

For the sake of convenience, we now discuss the morphological evolution together with the evolution of the area fraction of the polymer-rich phase shown in Fig. 10. It is seen from both Figs. 9(a) and 10 that the phase inversion process will happen earlier when ϕ_0 is higher. Certainly, the final values of the area fraction of the polymer-rich phase, which can be estimated through $\phi^e_{\rm area}=\phi_{e,{\rm pc}}\phi_0$ with $\phi_{e,{\rm pr}}$ the equilibrium composition of the polymer-rich phase, will be different. In comparison with the influence of M^0_b in Fig. 3, the time of phase inversion becomes more and more antecedent than the time of the concentration fluctuation amplification along with the decrease of ϕ_0. We think that this ''antecedent effect of phase inversion'' and the ''retardation effect'' of lower ϕ_0 may bring on MDP proposed by Tanaka [8]. For the sake of convenience, we summarize the features of the MDP described by Tanaka [16]. First, droplets are moving vigorously by Brownian motion, but they rarely coalesce even though they collide with each other. An unusually slow coarsening and unusual dependence of the coarsening rate on the quench depth are obtained in MDP. Second, in MDP, the size of droplets is smaller and more concentrated than that in usual phase separation, meanwhile the size distribution of droplets is very narrow. It is worth mentioning that the usual evaporation-condensation mechanism and Brownian-coagulation mechanism can play few roles in the coarsening dynamics of the MDP. In the similar experiments performed by Tanaka [8,9], the appearance of a moving droplet phase is only for dilute polymer solutions for deep quenching. Tanaka explained the mechanism of the MDP by regarding droplets as elastic gel balls, which may be in a ''dynamically stabilized state'' and not in thermodynamically stable state. Here we will give a more detailed analysis of the mechanism of MDP, and generalize the MDP and the network phase into a more universal class with only the distinction of kinetics. As shown in Fig. 9(a), for dilute polymer solutions, i.e., low ϕ_0, the phase inversion could occur implicitly since the concentration in the polymer-rich phase has not increased at the moment. Once the concentration fluctuation is amplified, the network has broken and shrunk to a polymer-rich droplet phase (i.e., MDP), which gives a wide berth from each other. This is more clearly seen for the case ϕ_0 equal to 0.08 in Fig. 9(b), in which N is set to 10 so as to approach lower ϕ_0 similar to real experimental system. With the increase of N the corresponding phase diagram becomes asymmetric and the critical temperature is raised, thus we adjust the quench depth $\chi=1.3$ to guarantee the deep quenching condition that is needed for the appearance of MDP. We also increase the intensity of the initial Gaussian random noise of ϕ to 10^{-2} so as to accelerate the evolution process of MDP. From Fig. 9(a) ($\phi_0=0.275$) and Fig. 9(b) we can see that the coarsening rate kept low and a condensed elastic gel ball formed due to the implicit phase inversion in the early stage. Then, the MDP appeared gradually and the growth rate of it became higher because the merging of solvent holes. At last the MDP, formed by the shrinking of the broken network, keep a certain distance between each other resulting in the eventual slow coarsening rate. The above physical picture could be also obtained from the tendency of F_a in Fig. 11. The retardation effect of the decrease of ϕ_0 is illustrated fairly in Fig. 12, in which the transition time for the phase inversion is determined the same way as in Fig. 4. From Fig. 13(a) we can see that the growth exponent α_1 is very small for the case of low ϕ_0 in the early and late stages, which coincide with the characteristics of MDP. It should be mentioned that the experimental results performed by Tanaka [8,9] and Haas and Torkelson [23] are consistent with our simulation results. The reason of small size and slow coarsening rate of the polymer-rich droplets in MDP can also be explained from the fact of the spatial constraint after the thin network structure is broken.

The retardation effect can also be seen from the growth exponent of the second peak maximum (k_{m2}), α_2 shown in Fig. 13(b). It is clearly seen from Fig. 13(b) that the growth exponent of the second peak α_2 increases along with the

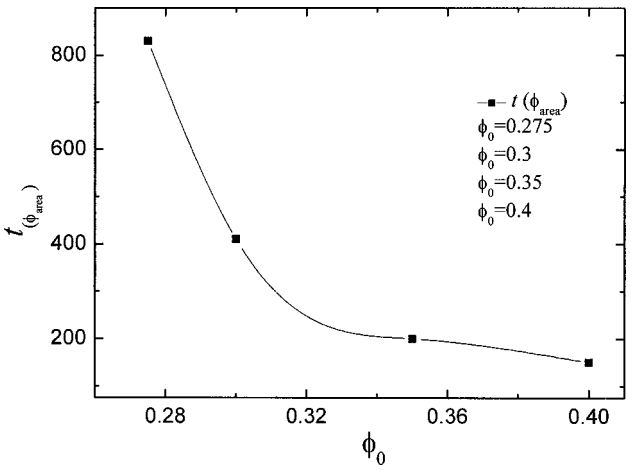

FIG. 12. The transition time for the phase inversion as a function of the average composition of polymer, ϕ_0. The transition time is defined in Fig. 3.

increase of ϕ_0 in the middle stage.

Figure 14 shows the average composition effect on the relaxation functions of bulk modulus. The general characteristic of this figure are quite similar to Fig. 8. The results agree with Fig. 10 and 11 quite well. By carefully looking at Fig. 14, it is seen that the slope of the first process increases with decrease of the average composition of polymer.

D. Further discussions on the dynamic phase diagram of a viscoelastic phase separation

Here we should mention that the dynamical diagram presented by Tanaka [16,24], in which a dynamical symmetry line (DSL) was introduced to determine the threshold composition required for the formation of a transient network, cf. Fig. 10 in Ref. [24]. On the left side of the DSL the MDP was observed, while a network domain structure was seen on the right side of the DSL. Near the DSL the bicontinuous pattern could be observed. Another feature of the dynamical diagram is that the MDP region becomes narrow in company with the increase of quenching depth. The above picture is very consistent with our results. It seems that the region near the DSL may be the transition region between MDP and phase inversion. In the region of forming network pattern, the phase inversion is prolonged and the network structure is maintained longer with the augmentation of ϕ_0 and M_b^0, especially in the case the complete breakup of network does not occur when F_α has reduced to the final equilibrium value. With increase of the quenching depth, F_α is increased and accelerated (the figures are not shown here for simplicity). However, F_α is decreased with decrease of ϕ_0. Thus, the phase inversion could be more easily observed for deep quenching at the same average composition, which results in the narrowing of the MDP region. In the case of deep quenching, except for the ''antecedent effects of phase inversion'' relative to the concentration fluctuation amplification, the origin of MDP through the usual phase inversion should be possible from the kinetics point of view. It is usually believed that, for deep quench, the asymmetric stress distribution between the polymer-rich and solvent-rich phases be-

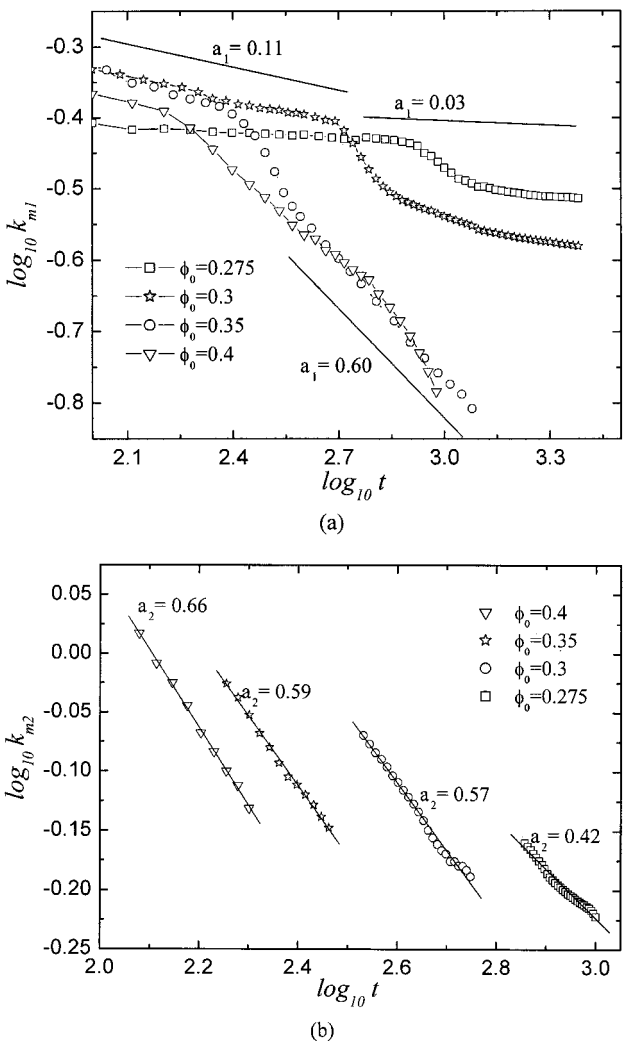

FIG. 13. (a) The growth exponent of the main scattering peak maximum as a function of the average composition of polymer, ϕ_0; (b) The growth exponent of the secondary scattering peak maximum.

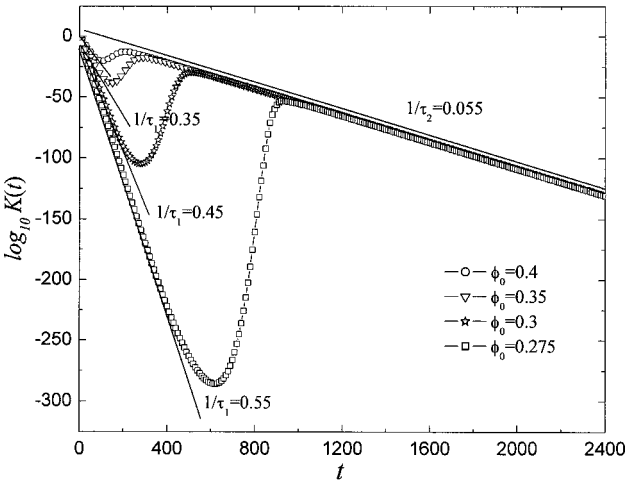

FIG. 14. The average polymer composition dependence of the relaxation functions of bulk modulus in the polymer-rich phase.

comes more prominent, which strongly restrains the augmentation of F_α and postpones the process of phase separation. As a result, the unusual phase inversion and then the MDP were observed. With increase of ϕ_0, the rate of the relaxation of dynamical asymmetry is also improved. The effect of the competence between two dynamic processes, i.e., the phase separation and the relaxation of dynamic asymmetry, is illustrated as following. For the case of low average composition, two dynamical processes are synchronously retarded and the relaxation of dynamic asymmetry becomes faster than the growth of concentration fluctuation. Therefore, the phase inversion occurred implicitly before the concentration in polymer-rich phase increased notably and thus formed MDP in comparison with the usual phase separation. For the case of intermediate average composition, the two dynamical rates are comparative and usual phase inversion is observed. For the case of high initial concentration, two dynamical processes are synchronously accelerated and the relaxation of dynamic asymmetry becomes slower than the growth of concentration fluctuation. Accordingly, the concentration in polymer-rich phase has reached the final equilibrium value before the disconnection of network (i.e., completely phase inversion) happened.

Now we would like to discuss the origin of dynamic phase diagram from the viewpoint of shifting of the apparent phase diagram including the dynamic effect [24,25]. When the stress term $\nabla \cdot \boldsymbol{\sigma}$ has been added to the apparent free energy, the phase diagram will be inclined. The extent of inclination of the apparent dynamic phase diagram depended on the relative contributions between $\nabla \cdot \boldsymbol{\sigma}$ and $\nabla \cdot \boldsymbol{\Pi}$, or the magnitude of modulus contrast $K(t) = M_b \exp(-t/\tau_b)$, namely, the extent of dynamical asymmetry. At first, the initial state in apparent phase diagram may fall into the right side of static composition symmetry line (SSL) or even into nucleation growth region, which may lead to the growth of the solvent-rich domains and initial ''frozen period.'' Consequently, the extent of the inclination of the apparent dynamic phase diagram decreases due to the relaxation of dynamical asymmetry. Then, the initial state originally on the right side of the apparent dynamic phase diagram may transform into the left side of SSL (i.e., polymer-rich droplet region), which gives birth to phase inversion. It should be stressed that this process is coupled with the enhancement of concentration fluctuation. The evolutions of the bulk modulus and the area fraction of the polymer-rich phase shown in Figs. 14 and 10 reveals that the reversion rate of the declined apparent dynamic phase diagram to the static phase diagram is faster than the concentration fluctuation amplification rate when the average composition is low. Thus, the MDPs are formed if the average composition is low. On the other hand, for the case of high average composition of the polymer, the relaxation of bulk modulus is slower than the evolution of the area fraction of the polymer-rich phase, so that the network structure could be maintained longer.

For the similar effect of M_b^0, the relaxation of dynamic asymmetry and the rate of concentration fluctuation amplification became slower when the dynamic asymmetry or M_b^0 are increased. Generally speaking, when M_b^0 increased, the extent of inclination of the apparent dynamic phase diagram increased and the reversion rate of it slowed down coupled with the retardation of concentration fluctuation amplification. Once M_b^0 increased to certain value for the case of high ϕ_0, the reversion rate becomes slower than the rate of phase separation, the network would be retained longer due to the exhaust of the thermodynamic force and the coupled stress force.

IV. SUMMARY

In this paper, the effects of relaxational bulk modulus and the average composition of polymers on the viscoelastic phase separation are investigated in detail. By comparing with the symmetric viscoelastic model, we have proved that the dynamical asymmetry is the premise of viscoelastic phase separation. It is also found that the relaxation of the dynamical asymmetry and the amplification of the concentration fluctuation are responsible for the appearance and evolution of the morphologies of viscoelastic phase separation. With increase of the bulk modulus M_b^0, the extent of initial dynamical asymmetry increased and the relaxation of it became slower coupling with the retardation of the concentration fluctuation amplification. For the case of $M_b^0 \sim 0$, namely, the case of dynamical symmetry, the characters of the usual phase separation are observed as expected. For the case of intermediate value of M_b^0, the phase inversion can be explicitly observed. As M_b^0 is further increased, the phase inversion is prolonged and the network structure retained longer. Especially in the case of higher $\phi_0 = 0.4$ and $M_b^0 = 5$, there is no evidence of the breakup of network into droplets (at least until $t = 2400$).

We have also investigated the average composition effect on the viscoelastic phase separation. It is found that, with the decrease of average composition of polymer, the relaxation of the bulk modulus becomes faster along with the retardation of the concentration fluctuation amplification. For the case of high average composition of the polymer, the relaxation of dynamical asymmetry becomes slower than the concentration fluctuation amplification, which also results in the retarded phase inversion and longtime network. For the case of intermediate average composition of polymer, the usual phase inversion is also observed. More interestingly, for the case of low average composition of polymer, the relaxation rate of dynamical asymmetry became faster than the amplification process of concentration fluctuation, which led to a MDP pattern. We now can conclude that the difference between the influence of the augmentation of M_b^0 and the decrease of ϕ_0 lies in the corresponding relaxation rate of dynamical asymmetry, which caused a so-called ''antecedent effect of phase inversion.'' Except that, we should also remind the reader that the retard effects with the decrease of ϕ_0 make observation of MDP easier in comparison with the acceleration effects of decrease of M_b^0.

Concerning the scattering function, we have found that the scattering function has two peaks for the case of viscoelastic phase separation, which agrees with the experimental results quite well [21]. The growth exponent of the main peak increased along with the increase of M_b^0 and approxi-

mately reached ~0.6 in the late stage. The growth exponent of secondary peak in the middle stage is also ~0.6, which also agrees with the experimental observations [21]. On the other hand, the growth exponent of the secondary peak decreased from ~0.66 to 0.42 with decrease of ϕ_0 from 0.4 to 0.275, in the intermediate stage. It seems to us that the shear relaxational modulus is not responsible for the formation of the network structure but the maintenance of it, which basically agrees with the observation of Tanaka [16].

Finally, we have to point out that the viscoelastic phase separation is quite complex, and further experimental and theoretical studies for understanding the kinetics and morphology in viscoelastic phase separation are highly desired.

ACKNOWLEDGMENTS

This work is subsidized by the Special Funds for Major State Basic Research Projects (G1999064800), NSF of China. Partial financial support from The Shanghai Commission of S&T is also acknowledged.

[1] P. G. de Gennes, J. Chem. Phys. **72**, 4756 (1980).
[2] M. Doi and A. Onuki, J. Phys. II **2**, 1631 (1992).
[3] A. Onuki, J. Phys. II **2**, 1505 (1992).
[4] A. Onuki and T. Taniguchi, J. Chem. Phys. **106**, 5761 (1997).
[5] V. Kumaran and G. H. Fredrickson, J. Chem. Phys. **105**, 8304 (1996).
[6] E. Helfand and G. H. Fredrickson, Phys. Rev. Lett. **62**, 2468 (1989).
[7] H. Tanaka, Phys. Rev. E **56**, 4451 (1997); **59**, 6842 (1999); T. Araki and H. Tanaka, Macromolecules **34**, 1953 (2001).
[8] H. Tanaka, Macromolecules **25**, 6377 (1992).
[9] H. Tanaka, Phys. Rev. Lett. **71**, 3158 (1993).
[10] H. Tanaka, Phys. Rev. Lett. **76**, 787 (1996).
[11] S. W. Song and J. M. Torkelson, Macromolecules **27**, 6389 (1994).
[12] D. Sappelt and J. Jäckle, Polymer **39**, 5253 (1998).
[13] R. Ahluwalia, Phys. Rev. E **59**, 263 (1999).
[14] N. Clarke, T. C. B. McLeish, S. Pavawongsak, and J. S. Higgins, Macromolecules **30**, 4459 (1997).
[15] Yi Cao, Hongdong Zhang, Zang Xiong, and Yuliang Yang, Macromol. Theory Simul. **10**, 314 (2001).
[16] H. Tanaka, J. Phys.: Condens. Matter **12**, 207 (2000), and references therein.
[17] T. Taniguchi and A. Onuki, Phys. Rev. Lett. **77**, 4910 (1996).
[18] H. Tanaka and T. Araki, Phys. Rev. Lett. **78**, 4966 (1997).
[19] C. Sagui, L. Piche, A. Sahnoune, and M. Grant, Phys. Rev. E **58**, 4654 (1998).
[20] P. G. de Gennes, *Scaling Concepts in Polymer Physics* (Cornell Univ. Press, New York, 1979).
[21] N. Kuwahara and K. Kubota, Phys. Rev. A **45**, 7385 (1992).
[22] J. H. Aubert, Macromolecules **23**, 1446 (1990).
[23] C. K. Haas and J. M. Torkelson, Phys. Rev. Lett. **75**, 3134 (1995).
[24] H. Tanaka, J. Chem. Phys. **100**, 5323 (1994).
[25] W. F. Busse, Phys. Today **17** (9), 32 (1964); J. Polym. Sci. A **5**, 1261 (1967).